ACCEPTED PAPER

Electrical and optical parameter-based numerical simulation of high-performance CdTe, CIGS, and CZTS solar cells

Galib Hashmi[1]*, Md. Shawkot Hossain[2], Masudul H. Imtiaz[3]

[1]*Institute of Energy, University of Dhaka, Bangladesh*
[2]*Department of Electronics and Communication Engineering, Institute of Science and Technology, National University, Bangladesh.*
[3]*Department of Electrical and Computer Engineering, Clarkson University, Potsdam, NY, USA*
E-mail: galib@du.ac.bd

Electrical and Optical Parameter-based Numerical Simulation of High-Performance CdTe, CIGS, and CZTS Solar Cells

Galib Hashmi[1*], Md. Shawkot Hossain[2] and Masudul H Imtiaz[3]

[1]Institute of Energy, University of Dhaka, Bangladesh
[2]Department of Electronics and Communication Engineering, Institute of Science and Technology,
National University, Bangladesh.
[3]Department of Electrical and Computer Engineering, Clarkson University, Potsdam, NY, USA
[*]E-mail: galib@du.ac.bd

ABSTRACT

The market for thin-film solar cells is gradually increasing and is expected to grow to 27.11 billion dollars by 2030. The most extensively researched thin film technologies based on simulation right now include solar cells made of Cadmium Telluride (CdTe), Copper Indium Gallium Selenide (CIGS), and Copper Zinc Tin Sulfide (CZTS). This work aims to use free software that does accurate simulation using the electrical and optical parameters (absorption coefficients) published in the literature. Moreover, to optimize efficiency, numerical simulation of all the solar cells has been done for different buffer layers (Cadmium Sulfide (CdS), Zinc Sulfide (ZnS)) and transparent conductive oxide (TCO) layers (Aluminum Zinc Oxide (AZO), and Indium Tin Oxide (ITO)). To assess the performance of the solar cells, changes have been made in the thickness of TCO layers and the alteration of doping concentrations of buffer layers and absorber layers. The simulation shows that 0.1 µm is the best TCO thickness. Furthermore, the AZO layer output outperforms the ITO layer in the simulation. It has also been investigated how employing a zinc telluride (ZnTe)-based back-surface reflector (BSR) layer will affect the results. This work includes representations of all the solar cell's open circuit voltage (Voc), short circuit current density (Jsc), maximum power (Pm), fill factor (FF), and photovoltaic efficiencies. The simulation's findings could be useful in the creation and comprehension of high-efficiency thin film solar cells.

Keywords: Cadmium Telluride (CdTe); Copper Indium Gallium Selenide (CIGS); Copper Zinc Tin Sulfide (CZTS); Thin Film Solar Cell (TFSC); WxAMPS

1. Introduction

The leading research on thin film technology of today is copper indium gallium selenide (CIGS), cadmium telluride (CdTe), and copper zinc tin sulfide (CZTS) solar cells. Since Shockley–Queisser limit has not been reached yet, there is still room for improvement for these solar cells. However, the fabrication of any of these solar cells is complex, and altering their parameters is time-consuming, difficult, and expensive. Moreover, proper laboratory and equipment are other important aspects of solar cell designing. Hence, simulation plays a vital role in solar cell design.

A review of the literature on solar cell simulation [1-18] reveals that a variety of simulation software is used for solar cell design, and the most popular computer programs for simulating solar cells are SCAPS-1D (Solar Cell Capacitance Simulator- One Dimension) and Silvaco-Atlas Technology Computer-Aided Design (TCAD) software. Since TCAD is commercial software, there are few opportunities for everyone to utilize it, and therefore has not been used in this research. Although the SCAPS is free software, the optical parameters (absorption coefficients) are given by default. Because the default optical parameters are not experimentally obtained values, using them could result in inaccurate simulations.

Thus, in this research work, one of the main goals is to use free software where the electrical and optical parameters found in the literature can be used for accurate simulation of CdTe, CIGS, and CZTS solar cells. In WxAMPS (Widget Provided Analysis of Microelectronic and Photonic Structures) software, optical parameters are not given by default, and it is free and easy-to-operate software; thus, it has been used for all kinds of thin film solar cell simulation.

So far, the recorded laboratory efficiency in thin film technology for CIGS, CdTe, and CZTS solar cells is 23.35%, 21.0%, and 10.0%, respectively [19]. The CdTe solar cell simulation study shows that the typical solar cell structure is ZnO/CdS/CdTe, and efficiency ranges between 17% and 23% [20-24]. Whereas ZnO/CdS/CIGS is the most common solar cell structure seen in the CIGS solar cell modeling study, and its efficiency ranges from 16.39% to 21.3% [1-6, 25]. ZnO/SnS$_2$/CZTS or ZnO/ CdS /CZTS solar cell structure has been observed in the CZTS solar cell simulation study, with efficiency spanning between 10.69% and 11.58% [7-12].

As seen from the reported simulation work, in most cases, the ZnO serves the purpose of both transparent conductive oxide (TCO) and the window layer for CdTe, CIGS, and CZTS solar cells [1-12, 19-25]. However, in this work, indium tin oxide (ITO) and aluminum zinc oxide (AZO)

has been used as a transparent conductive oxide (TCO) layer. The reason for choosing ITO and AZO is that they are widely used in commercial applications and can reduce energy loss by up to 30% [13]. Furthermore, the dispute over AZO vs. ITO as TCO is still ongoing; another goal of this research is to see which TCO performs well for CdTe, CIGS, and CZTS solar cells. Therefore, both AZO and ITO have been individually used as TCO layers in solar cell simulations.

Moreover, simulation also assists the researchers in studying and observing the behaviors and provides insightful knowledge about how the devices operate. Additionally, simulation offers the resources to optimize the solar cell, which is the final objective of this study. Therefore, the thickness of TCO layers and alteration of doping concentrations of buffer layers and absorber layers have been done in the simulation to obtain optimum efficiency for CIGS, CdTe, and CZTS solar cells. In addition, simulations have been conducted with three types of absorber layers (CdTe, CIGS, and CZTS layer) to differentiate from others' work and for better understanding via comparison. Metal sulfides are a significant type of semiconductor in which the bandgap can be somewhat modified by simply manipulating the particle sizes, without changing the chemical composition [26]. Among metal sulfides, cadmium sulfide (CdS) has direct wide-bandgap properties and the literature review shows it is the most widely used buffer layer in thin-film solar cells. The study also shows zinc sulfide (ZnS) is a promising material having also direct wide-bandgap properties and can be used as an alternative to cadmium sulfide (CdS) buffer layer. In light of the aforementioned reasons, the sulfide-based materials CdS and ZnS have been utilized to simulate the three different types of solar cells.

In a semiconductor, there are various kinds of recombination mechanisms. One of the recombination mechanisms is more effective than others depending on how semiconductors are used and the prevailing conditions. Radiative and non-radiative recombination are two different types of recombination that occur in semiconductors. Non-radiative recombination can be further classified into: recombination through defects (shockley-read-hall recombination (SRH)), auger recombination, and surface recombination. Furthermore, recombination is generally categorized according to the region of the solar cell where it occurs. The main locations of recombination are often at the surface (surface recombination) or in the bulk of the solar cell (bulk recombination). Another area where recombination can take place is the depletion region (depletion region recombination) [27-28].

Both the forward bias injection current (and accordingly open-circuit voltage) and the current collection (and consequently the short-circuit current) are impacted by recombination losses. Surface and bulk recombination should both be reduced to make it easier for the P-N

junction to capture all of the light-generated carriers. In the recombination process, back contact has a greater impact since it has a larger surface area with the semiconductor in the solar cell. Reducing surface recombination velocity (SRV) and the recombination process can be accomplished by passivating the rear contact or producing a strong electric field there. The generated carriers can be immediately swept by a strong electric field at the rear contact. The semiconductor region in contact with the metal can be heavily doped to produce an electric field. A heavily doped layer called the back-surface reflector (BSR) layer, at the rear end (just before back contact) can create a surface field that helps in improving the efficiency of the solar cell. In this work, ZnTe material has been used as the BSR layer for CdTe and CIGS solar cells. The reason for selecting ZnTe as the BSR layer is that it is the only material whose experimentally obtained absorption coefficient value has been found in the literature. The performance of with and without zinc telluride (ZnTe) back-surface reflector (BSR) layers has also been investigated. All the observed results, including open circuit voltage (V_{OC}), short circuit current density (J_{SC}), maximum power (P_m), fill factor (FF), and efficiency (η) of different solar cells, have been discussed in this paper.

2. Thin Film Solar Cell (TFSC)

A solar cell (also called a photovoltaic cell, as shown in Fig. 1) is an electrical device that converts the energy of light directly into electricity by the photovoltaic effect [14]. The photovoltaic effect is the mechanism through which a photovoltaic cell produces a voltage when exposed to light or other forms of radiant energy [15].
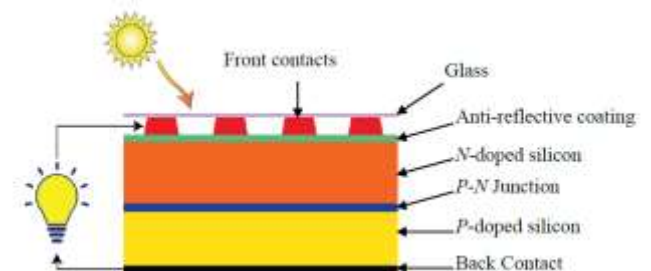

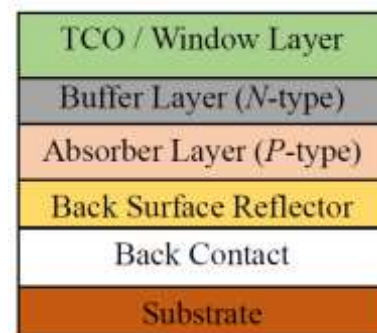**Fig. 1.** Basic Structure of a Silicon Solar Cell.

Fig. 2. The basic structure of a thin film solar cell where TCO and window layer are the same.

2

A thin film solar cell is a solar cell whose thickness varies from a few micrometers to a few nanometers and is constructed by depositing some thin layers consecutively. A general structure of a thin film solar cell is depicted in Fig. **2**. A thin film solar cell consists of different layers. Such as front contact / Transparent Conducting Oxide (TCO), window layer, buffer layer, absorber layer, back surface reflector (BSR), back contact, and substrate. The TCO and window layer can be separate or the same, as shown in Fig. **2** and Fig. **3**. Each layer has a specific function, and these layers are described briefly in the following section.
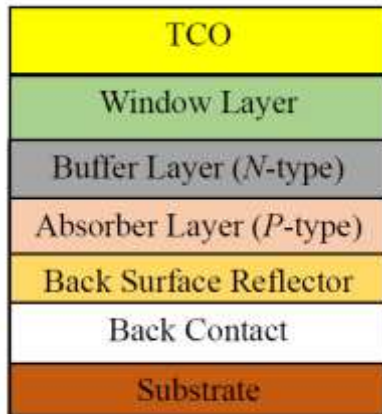

Fig. 3. The basic structure of a thin film solar cell where TCO and window layer are separate layers.

Front contact is the topmost layer of the thin film solar cell. The main function of this layer is to collect the current produced by the cell and serve it to an outer circuit or load. 1st generation solar cell has opaque grid finger front contacts. Whereas, in 2nd generation solar cells (Thin Film), the front contact is designed differently. The front contact is a transparent conductive oxide (TCO) layer. The conductive oxide serves the same purpose as the first generation's front contact, and its transparency allows light to enter the TFSC. Furthermore, the TCO is transparent, acting like a window of the solar cell through which the majority of the light enters. For this reason, it is called the window layer also. As a result, the TCO layer can function as both the window and the TCO layer at the same time (as shown in Fig. **2**, or they can be distinct layers (as shown in Fig. **3**. When the transparency of the TCO layer increases, the resistance also increases proportionally. The resistance of the TCO layer needs to be low because of the current collection from the buffer layer. To trade-off between transparency and conductance, sometimes TCO and window layers are separated to improve the overall performance of the solar cell. It is to be noted that the bandgap of the window layer must be high for greater light trapping and absorption of high-energy photons. The cell absorbs a great amount of light in this layer. Under the window layer is the buffer layer. The buffer layer, in general, is an N-type semiconductor material, which along with the P-type absorber layer, forms the P-N junction of

TFSC. The buffer layer is named so like this because it adjusts the bandgap matching between the absorber layer and the window layer. The doping concentration of a buffer layer must be high so that the number of minority carriers is reduced, and as a result, recombination can be minimized.

Recombination on this layer degrades the working ability of the solar cell. The absorber layer absorbs the low-energy photon as the bandgap of this semiconductor material is low. Generally, the absorber layer is a P-type semiconductor material with a higher contribution from photo-generated electron-hole (e-h) pairs [16]. Furthermore, the thickness of this layer is much higher than that of the other layers used in the solar cell. Not all TFSC architectures have the back-surface reflector (BSR) layer. In recent years, a back surface reflector (BSR) layer has been used to improve the performance of back contact and reduce the recombination in the structure. The essential role of this layer is to confine the photogenerated minority carriers and ensure it is close enough to reach the P-N junction so that the current can be proficiently collected [13, 17]. Using the back contact layer, a full path for the current carrying circuit is made and used for current collection from the cell. It is deposited on the substrate layer and makes contact with the back surface reflector (BSR) layer or absorber layer. On the substrate, the consecutive layers are deposited. The substrate can be glass, plastic, etc. soda-lime glass (SLG) is generally used as a substrate in TFSC.

2.1 Types of Thin Film Solar Cells (TFSCs)

In TFSC technology, there are different types of solar cells. These solar cells are named after the material used in the absorber layer. The first type of TFSC is an amorphous silicon solar cell. This type of TFSC uses a bulk amount of silicon. However, thin film technology has evolved to reduce the cost, and many solar cells, like CdTe, CIGS, CZTS, etc., have been designed successively. This research has simulated and optimized CdTe, CIGS, and CZTS TFSCs. Thus, some information about each of these cells is discussed in the following section.

2.1.1 Cadmium Telluride (CdTe) Solar Cell

Cadmium Telluride (chemical formula: CdTe) is today's second most utilized solar cell technology. The first is still 1st generation silicon solar cell. CdTe is a suitable material for solar cell operation. Because it has a direct bandgap of 1.45 eV for AM 1.5 solar spectrum and is nearly optimal for converting sunlight into electricity [18]. Furthermore, one of the great advantages of CdTe solar cells is it is a low-cost manufacturing technology. Nonetheless, the main problem with CdTe solar cells is their toxicity. Cd is harmful to the environment. However, toxicity tests reveal that CdTe is less harmful than elemental cadmium (Cd). The Ames mutagenicity test results for CdTe are negative, and it has minimal acute inhalation, oral, and aquatic toxicity. According to the results that were reported to the

3

European Chemicals Agency (ECHA), CdTe is no longer categorized as dangerous to aquatic life or harmful when it comes in contact with the skin. It has been discovered by researchers from the Brookhaven National Laboratory of the U.S. Department of Energy that the widespread usage of CdTe PV modules poses no hazards to human health or the environment [29]. As CdTe solar cell poses no serious threat and it is still widely used, therefore, CdTe solar cell simulation has been done.

It should be mentioned that the CdTe fabrication process must take place in a controlled environment; otherwise, toxic Cd emissions may be produced during the CdTe production process. Thus, much research is running to find an alternative to the CdTe solar cell and therefore, simulations of CIGS, and CZTS have been done as an alternative to CdTe solar cells. By using cadmium sulfide (CdS) as a buffer layer, the toxicity of the buffer layer CdTe solar cell is reduced further as the CdS material is less toxic than the Cd material alone. Currently, much research is running to find an alternative to the CdS buffer layer to reduce the toxicity effect. Table **1** lists the most prominent current research materials with thickness for CdTe solar cells.

2.1.2 Copper Indium Gallium Selenide (CIGS) Solar Cell

Copper Indium Gallium Selenide (CIGS) is another kind of TFSC where CIGS is used as an absorber layer. The CIGS material is a solid solution of copper indium selenide (CIS) and copper gallium selenide. It has a chemical formula of $CuIn(1-x)Ga(x)Se_2$. Where the value of x can vary from 0 (pure copper indium selenide) to 1 (pure copper gallium selenide). The bandgap of CIGS material varies continuously with x from about 1.0 eV (for copper indium selenide) to about 1.7 eV (for copper gallium selenide). As CIGS film acts as a direct bandgap semiconductor. CIGS material is used instead of CdTe as an absorber layer; CIGS has an advantage over CdTe in toxicity aspects. Nevertheless, the toxic effect still has not been completely removed as, in general, CdS is used as a buffer layer. However, alternative materials are used as a substitute for CdS nowadays. Summarized thickness, materials, and associated layers of CIGS solar cell are given away in Table **1**.

Table 1. General List of Different TFSC with Associated Layers, Thickness & Materials

Layers name	t	CdTe Solar Cell Material list	CIGS Solar Cell Material list	CZTS Solar Cell Material list
Window/ TCO	(0.1 to 1.0) µm	**ITO**/CTO/FTO/ZnO/ SnO₂/ZnMgO/ **AZO**	**ITO**/CTO/FTO/ZnO/ SnO₂/ZnMgO/**AZO**	**ITO**/CTO/FTO/ZnO/ SnO₂/ZnMgO/ **AZO**
Buffer layer	(20-100) nm	**CdS**/ZnSe/ZnCdS/In₂S₃/ **ZnS**/In₂Se₃	**CdS**/ZnSe/In₂S3/ **ZnS**/ZnO/MgZnO	**CdS**/ZnSe/ZnCdS/In₂S₃/ **ZnS**/In₂Se₃
Absorber layer	(1-6) µm	**CdTe**	**CIGS**	**CZTS**

		CdTe Solar Cell	CIGS Solar Cell	CZTS Solar Cell
BSR	(0.1-1) µm	**ZnTe**/Sb₂Te₃	**ZnTe**/Sb₂Te₃	-
Back Contact	(0.5-1.0) µm	Ag/Mo/Al	Ag/Mo/Al	Ag/Mo/Al
Substrate layer	(1-2) µm	Glass/plastic	Glass/plastic	Glass/plastic

Footnote: t - represents thickness.

2.1.3 Copper Zinc Tin Sulfide (CZTS) Solar Cell

One of the critical issues with CdTe and CIGS-based solar cells is the less availability of tellurium and indium on earth. To solve this problem, Copper Zinc Tin Sulfide (CZTS) material has drawn the attention of researchers as an alternative absorber layer. Furthermore, CZTS is a non-toxic, low-cost, earth-abundant material having reasonable electrical and optical properties. The chemical formula of CZTS is Cu_2ZnSnS_4. CZTS also has a direct and tunable band gap (Eg ~ 1.45 eV- 1.6 eV). Yet detoxification of Cd from the CdS buffer layer is still an issue for its advancement. As a result, research on CZTS solar cells is currently ongoing. Parameters of associated layers and materials of CZTS solar cells are presented in Table **1**.

3. Simulation

WxAMPS is a popular simulation software for the modeling of thin-film solar cells. In the software, the solar cells are modeled as having a size of 1cm × 1cm and an input power of 100 mW/cm². Also taken into consideration are the standard values of air mass 1.5G and room temperature 300K (25°c).

Specific electrical parameter values for each layer must be included in the simulation to operate accurately. The values of the electrical parameters for particular materials are stated in Table **2**.

Table 2. The Physical Parameters of Different Layers

Parameters	CdTe [30-31]	CIGS [32-35]	CZTS [14,36]	CdS [30-34]	ZnS [7,33, 37]	AZO [34]	ITO [7]	ZnTe [34]
W (µm)	1-6	1-4	1-4	0.02-0.1	0.02-0.1	0.1-1	0.1-1	0.1-1
Eg (eV)	1.50	1.13	1.5	2.42	3.5	3.30	3.6	2.26
εr	9.4	13.6	10	10	10	9.0	10	9.67
χe (eV)	4.6	4.41	4.5	4.3	4.5	4.35	4.1	3.50
µn (cm²/vs)	320	100	100	100/350	50	100	50	330
µp (cm²/vs)	40	25	25	25/50	20	25	75	80
Nc (cm⁻³)	8×10¹⁷	2.2×10¹⁸	2.2×10¹⁸	2.2×10¹⁷	1.5×10¹⁸	2.2×10¹⁸	2.2×10¹⁸	7×10¹⁶
Nv (cm⁻³)	1.8×10¹⁹	1.8×10¹⁹	1.8×10¹⁹	1.8×10¹⁸	1.8×10¹⁸	1.8×10¹⁹	1.8×10¹⁹	2×10¹⁹
ND (cm⁻³) Ref. Value	0	0	1×10¹	1×10¹⁷	5×10¹⁵	1×10¹⁸	1×10¹⁹	0
NA (cm⁻³) Ref. Value	2×10¹⁶	2×10¹⁶	2×10¹⁴	0	0	0	0	1×10¹⁸

Footnote: Thickness - W (µm), Bandgap - Eg (eV), Relative Permittivity - εr, Electron affinity - χe (eV), Electron mobility - µn (cm²/vs), Hole mobility - µp (cm²/vs), Conduction band density - Nc (cm⁻³), Valence band density

- N_v (cm^{-3}), Donor concentration - N_D (cm^{-3}), Acceptor concentration - N_A (cm^{-3})

Some simulator settings can be modified, but only to a certain extent. Changes can be made to the layer's thickness and the N- or P-type material's doping concentrations. These factors have been changed to produce a better outcome. Optical parameter values (wavelengths and their respective absorption coefficients) have been inputted alongside electrical parameters. Table **3** contains the values for the optical parameters taken from the literature [37-45].

Table 3. Wavelength and their Respective Absorption Coefficient

λ (nm)	CdS [37] α (m^{-1})	CdTe [37] α (m^{-1})	ZnTe [38] α (m^{-1})	AZO [37] α (m^{-1})	CZTS [39-40] α (m^{-1})	ZnS [41] α (m^{-1})	CIGS [42] α (m^{-1})	ITO [42-45] α (m^{-1})
320	1.49×10^7	6.94×10^7	6.32×10^7	6.06×10^6	-	1.17×10^7	4.03×10^7	6.66×10^6
360	1.26×10^7	4.52×10^7	3.70×10^7	4.84×10^5	-	1.88×10^6	3.51×10^7	2.30×10^6
400	1.06×10^7	2.22×10^7	1.43×10^7	3.62×10^4	5.46×10^6	2.51×10^5	3.61×10^7	9.0×10^5
440	9.05×10^6	1.40×10^7	1.01×10^7	2.46×10^4	5.38×10^6	8.56×10^4	2.72×10^7	3.95×10^5
480	7.23×10^6	1.17×10^7	7.67×10^6	2.61×10^4	5.24×10^6	2.61×10^4	1.87×10^7	1.99×10^5
520	7.12×10^5	9.66×10^6	5.20×10^6	3.19×10^4	5.19×10^6	-	1.41×10^7	1.24×10^5
560	5.14×10^2	7.86×10^6	2.19×10^6	4.00×10^4	5.18×10^6	2.24×10^4	1.13×10^7	1.02×10^5
600	0.007364	6.44×10^6	1.47×10^6	5.00×10^4	5.26×10^6	4.18×10^4	1.02×10^7	1.04×10^5
640	4.35×10^{-13}	5.38×10^6	1.20×10^6	6.19×10^4	5.33×10^6	3.92×10^4	8.89×10^6	1.19×10^5
680	$(-)2.54 \times 10^{-14}$	4.42×10^6	1.02×10^6	7.58×10^4	5.09×10^6	9.24×10^4	7.47×10^6	1.37×10^5
720	2.0×10^{-14}	3.37×10^6	8.82×10^5	9.19×10^4	5.21×10^6	1.04×10^5	6.71×10^6	1.61×10^5
760	3.87×10^{-25}	2.30×10^6	7.72×10^5	1.10×10^5	5.24×10^6	1.15×10^5	6.35×10^6	1.85×10^5
800	$(-)2.69 \times 10^{-14}$	1.30×10^6	6.84×10^5	1.31×10^5	5.26×10^6	1.41×10^5	5.65×10^6	2.12×10^5

Footnote: Wavelength – λ (nm), Absorption coefficients - α (m^{-1})

Table **1** shows that materials like Ag, Cu, Mo, or Al can be used as back contact. But in this work, no back contact has been used in the simulation as WxAMPS simulation software does not offer any option to provide back contact. But in real life scenario, there must be a back contact for the current collection from the device. Furthermore, substrate selection is also not possible in WxAMPS software. The substrate is a material where the consecutive layers are deposited. It can be glass, plastic, etc. It is recommended to use soda-lime glass (SLG) as substrate in the thin film. Because SLG is slightly different from normal glass. When SLG is used as a substrate, the sodium ions diffuse into the absorber layer and improve the working capability of the solar cells. The simulations have been done for only front contacts, buffer layers, absorber layers, and BSRs.

The thickness range of the absorber layer, buffer layer, and BSR are presented in Table **1** (which has been obtained from the literature). For simplification, in all of the modeling, the thickness of the absorber layer, buffer layer, and BSR has been maintained at 2 μm, 0.02 μm, and 1 μm, respectively. The thickness optimization of these layers has not been done in this study and is kept for future work. But

to find the best TCO with the best thickness, thickness variations with aluminum-doped zinc oxide (AZO) and indium tin oxide (ITO) have been carried out in the range of 0.1 μm - 1.0 μm for all the solar cells. Moreover, cadmium sulfide (CdS) and its alternative zinc sulfide (ZnS) have been used as buffer layers. ZnTe has been utilized as the BSR for CdTe and CIGS solar cells, except for the CZTS solar cell (due to an unexpected error in simulation). In this simulation work, all the combinations used for CdTe, CIGS, and CZTS solar cells and their respective outcomes have been disclosed in the results and discussion section.

4. Results

4.1 Impacts of Thickness Variation of Transparent Conductive Oxide (TCO) Layers & Back-Surface Reflector (BSR)

4.1.1 CdTe Solar Cell

The four distinct TCO and buffer layer configurations for CdTe solar cells with BSR are AZO/CdS/CdTe/ZnTe, AZO/ZnS/CdTe/ZnTe, ITO/CdS/CdTe/ZnTe, and ITO/ZnS/CdTe/ZnTe respectively. In addition, four other unique combinations exist without the ZnTe BSR. The efficiency of these eight configurations' solar cells with and without ZnTe BSR is shown in Fig. **4**.
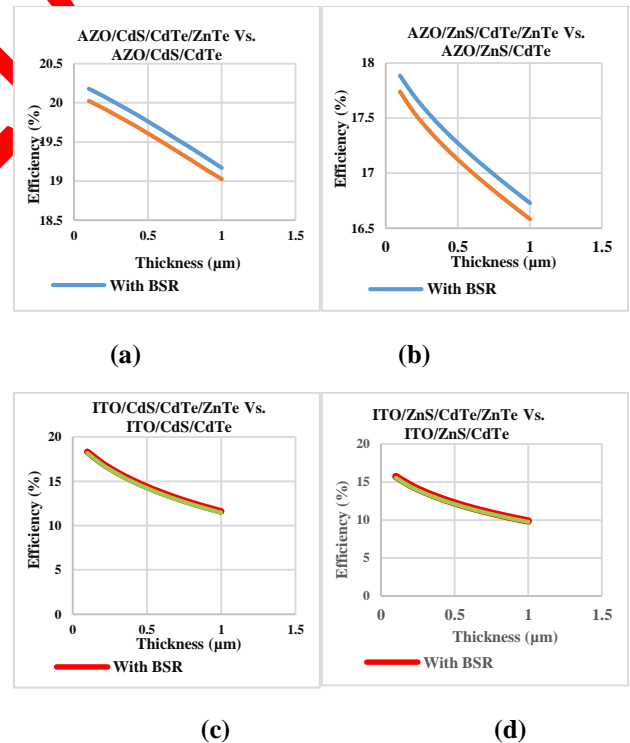
(a) **(b)**

(c) **(d)**

Fig. 4. TCO Thickness Variation with Efficiency for CdTe Solar Cell (a) AZO/CdS/CdTe/ZnTe (With BSR) Vs. AZO/CdS/CdTe (Without BSR) (b) AZO/ZnS/CdTe/ZnTe (With BSR) Vs. AZO/ZnS/CdTe (Without BSR) (c) ITO/CdS/CdTe/ZnTe (With BSR) Vs. ITO/CdS/CdTe (Without BSR) (d) ITO/ZnS/CdTe/ZnTe (With BSR) Vs. ITO/ZnS/CdTe (Without BSR).

It has been observed that the ZnTe BSR layer is slightly more efficient than without the ZnTe BSR layer for all combinations of CdTe solar cells. This is because the BSR layer reflects the incident light back to the absorber layer of the solar cell, thus extending the light path and causing the "light trapping effect" [46]. However, very little increase in efficiency is observed with BSR solar cells than without BSR solar cells, and it is in the range of 0.77% to 1.25%.

TCO thickness variation for CdTe solar cells with BSR is shown in Fig. **5** (As the solar cells with BSR have marginally greater performance than those without BSR solar cells, for this reason, the without BSR solar cells are not shown in this instance). To find out the optimum thickness of the TCOs (AZO and ITO), the thicknesses have been varied from 0.1 to 1.0 μm.

From the simulation, it can be seen that for each case of the respective TCO, 0.1 μm thickness has the highest efficiency. Whenever the thickness of TCOs is increased from 0.1 to 1 μm, the consequences are always associated with a reduction in efficiency. This is because when the thickness increases, the sheet resistance increases, and thus the overall conductivity decreases. The experimental study agrees that if the sheet resistance increases, then the overall conductivity also decreases [47]. However, it is also seen from the experimental study that low thickness does not always have the best value. Because when a layer thickness is minimized, many complications arise, and in this simulation, those factors have not been considered.
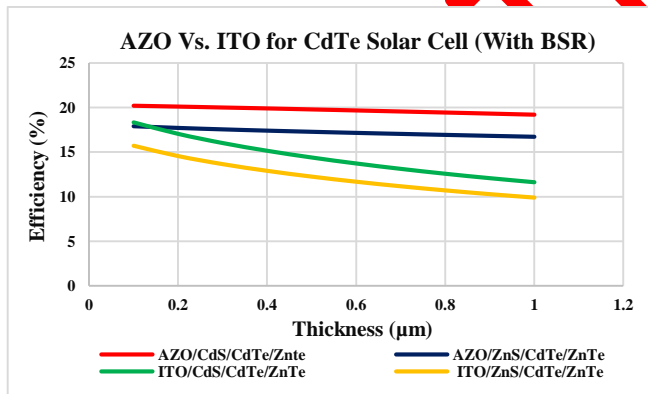

Fig. 5. TCO Thickness Variation for CdTe Solar Cell.

The Al-doped ZnO (AZO) thin films have less change in efficiency due to thickness variations than the indium tin oxide (ITO), as shown in Fig. **5**.

The reason is due to the alteration of the thickness; the variation in sheet resistance is low for AZO in comparison to ITO, where sheet resistance changes considerably. With 0.1 μm thick TCO, the AZO/CdS/CdTe/ZnTe solar cell attained the best efficiency of 20.179%, and the AZO/ZnS/CdTe/ZnTe solar cell came in second with 17.88% efficiency.

4.1.2 CIGS Solar Cell

Simulating a CIGS solar cell just requires replacing the CdTe absorber layer of a CdTe solar cell with a CIGS absorber layer. Similar to CdTe solar cells, there are four TCOs and buffer layers with BSR for CIGS solar cells, and they are called AZO/CdS/CIGS/ZnTe, AZO/ZnS/CIGS ZnTe, ITO/CdS/CIGS/ZnTe, and ITO/ZnS/CIGS/ZnTe, respectively. Furthermore, four other separate combinations also exist without the ZnTe BSR.

In Fig. **6**, the performance of the CIGS solar cells in these eight combinations with and without ZnTe BSR is depicted. Similar results to those of the CdTe solar cell have been found here. The results demonstrate that, for all combinations of CIGS solar cells, the BSR layer is slightly more effective than the BSR layer alone. The increase in efficiency of BSR solar cells over those without BSR ranges from 0.16% to 0.55%. It is expected that by reducing the thickness of the ZnTe BSR layer efficiency of solar cells can be increased for both CdTe and CIGS solar cells but has not been done in this paper. So it is proposed as the future work of this research.
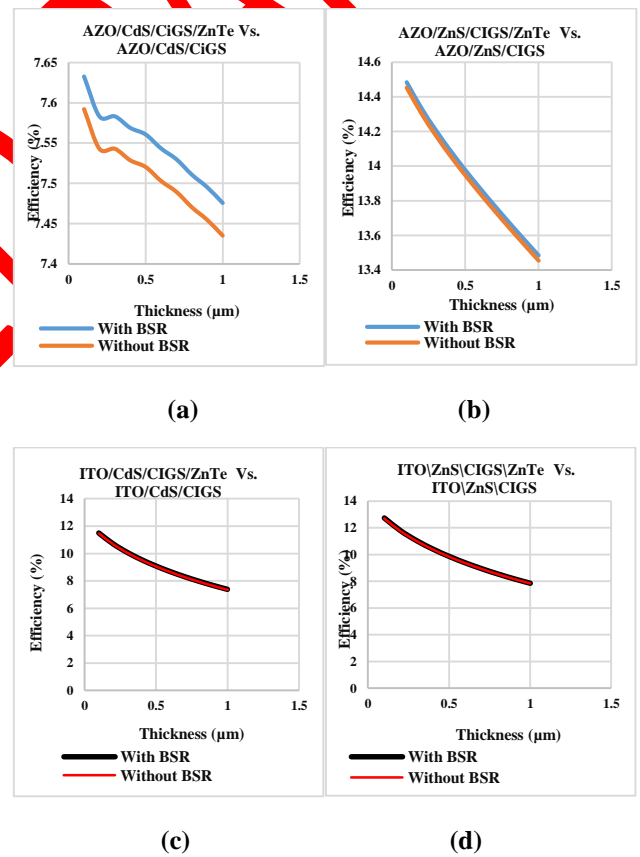

(a) **(b)**

(c) **(d)**

Fig. 6. TCO Thickness Variation with Efficiency for CIGS Solar Cell (a) AZO/CdS/ CIGS /ZnTe (With BSR) Vs. AZO/CdS/ CIGS (Without BSR) (b) AZO/ZnS/ CIGS /ZnTe (With BSR) Vs. AZO/ZnS/ CIGS (Without BSR) (c) ITO/CdS/ CIGS /ZnTe (With BSR) Vs. ITO/CdS/ CIGS (Without BSR) (d) ITO/ZnS/ CIGS /ZnTe (With BSR)Vs. ITO/ZnS/ CIGS (Without BSR).

Note: In Fig. 6. **(c)** and **(d)** are quite near to each other. It may be difficult to understand if printed in black and white.
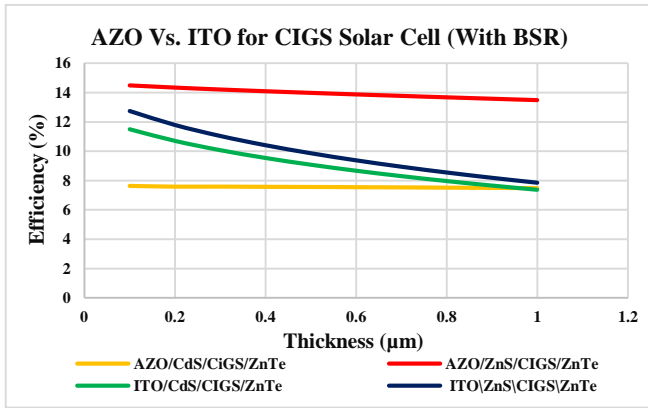
Fig. 7. TCO Thickness Variation for CIGS Solar Cell.

Fig. **7** depicts the variation in TCO Thickness for CIGS solar cells with BSR (Here, only the solar cells curves with BSR are shown because these cells have slightly better efficiency than the solar cells without BSR). In all of the TCO scenarios, it is found from the modeling of CIGS solar cells that the thickness of 0.1 μm has the maximum efficiency. Analogous thickness observations have been made of CdTe solar cells. In addition, Fig. **7** also depicts that, as thickness increases from 0. 1 to 1.0 μm, efficiency decreases.

Furthermore, Fig. **7** shows that AZO thin films exhibit less efficiency change due to thickness variation than ITO thin films. The two most efficient CIGS solar cells are AZO/ZnS/CIGS/ZnTe and ITO/ZnS/CIGS/ZnTe, both of which have 0.1 μm thick TCO and efficiency levels of 14.48% and 12.75%, respectively.
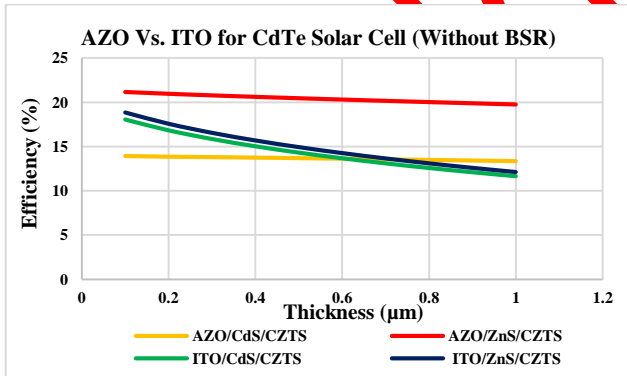
4.1.3 CZTS Solar Cell

Fig. 8. TCO Thickness Variation for CZTS Solar Cell.

As stated earlier, the ZnTe as the BSR layer for CZTS solar cells has been left out of this study, due to an unexpected error that occurred when it was used in the simulation. An alternative BSR layer for CZTS solar cells may be Copper telluride (Cu$_2$Te). Simulation has been performed (not shown or discussed in the paper) and it works with CZTS solar cells. The consequence of thickness variation of AZO and ITO without BSR is shown in Fig. **8**. On every occasion, an increase in thickness from 0.1 to 1 μm results declination in the efficiency of the TCOs. Once again, compared to the ITO layer, the AZO layer shows less

efficiency change due to thickness variation. The top two combinations, with 0.1 μm TCO thickness, are AZO/ZnS/CZTS and ITO/ZnS/CZTS, having efficiency values of 21.15% and 18.86%, respectively.

4.2 Impacts of Doping Concentrations

4.2.1 CdTe Solar Cell

As previously mentioned, for all simulations, the buffer layer, absorber layer, and BSR layer thicknesses have been set to 0.02 μm, 2 μm, and 1 μm, respectively.

Additionally, section 4.1 shows that the optimal TCO thickness is always 0.1 μm; hence this value has been chosen for the remainder of the CdTe, CIGS, and CZTS solar cell simulations. Furthermore, using the information from Table **2**, the four combinations have been simulated, and the result Voc, Jsc, FF, Pm, and η (highlighted in blue color) are tabulated in Table **4**.

Moreover, depending upon the material, the doping concentrations of P-type (absorber layer) & N-type (buffer layer) have been changed in the following ranges, 2×10^{12} - 2×10^{20}, 1×10^{12} - 1×10^{20} and 4×10^{12} - 5×10^{20}. The optimum doping concentrations and associated Voc, Jsc, FF, Pm, and η (highlighted in red color) values of the four combinations are represented in Table **4**.

Table 4. Voc, Jsc, FF, Pm, and η of CdTe Solar Cell

Dc of P-type CdTe (cm^{-3})	Dc of N-type (cm^{-3})	Jsc (mA/cm^2)	Voc (V)	P$_m$ (mW /cm^2)	FF (%)	η (%)
AZO/CdS/CdTe/ZnTe						
2×10^{16}	1×10^{17}	28.04	0.98	20.18	73.56	20.18
2×10^{15}	1×10^{20}	30.09	0.92	22.51	80.91	22.51
AZO/ZnS/CdTe/ZnTe						
2×10^{16}	5×10^{15}	28.67	0.98	17.88	63.64	17.88
2×10^{16}	4×10^{19}	29.14	0.98	20.19	70.70	20.19
ITO/CdS/CdTe/ZnTe						
2×10^{16}	1×10^{17}	24.91	0.972	18.32	75.63	18.32
2×10^{12}	1×10^{17}	28.36	0.97	19.92	72.43	19.92
ITO/ZnS/CdTe/ZnTe						
2×10^{16}	5×10^{15}	25.39	0.976	15.72	63.44	15.72
2×10^{16}	5×10^{18}	25.61	0.98	16.75	66.72	16.75

Footnote: Dc is donor concentration, J$_{SC}$ is short circuit current density, Voc is open circuit voltage, Pm is maximum power, FF is the fill factor, and η is efficiency.
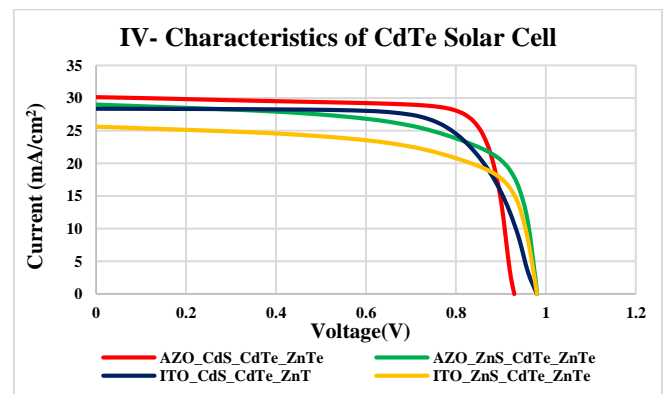

Fig.**9**. IV- Characteristics of CdTe Solar Cell

The simulation has demonstrated how changing doping concentration has an impact on solar cell efficiency. The optimal doping concentration has been taken into account when drawing the I-V curves of all four combinations of CdTe solar cells (as shown in Fig. **9**). The AZO/CdS/CdTe/ZnTe solar cell has the best efficiency of 22.51% out of the four combinations. The open circuit voltage (Voc), short circuit current density (Jsc), maximum power (Pm), fill factor (FF), and efficiency of AZO/CdS/CdTe/ZnTe solar cell are respectively 0.92 V, 30.09 mA/cm², 22.51 mW/cm², 80.91%, and 22.51%. One intriguing finding is that, after optimization, the AZO layer outperforms the ITO layer in CdTe solar cells.

4.2.2 CIGS Solar Cell

For the simulation of the CIGS solar cell, the TCO, buffer layer, absorber layer, and BSR layer thicknesses have been set to 0.1 μm, 0.02 μm, 2 μm, and 1 μm, respectively.

In addition, using the data from Table **2**, the four BSR combinations (discussed in section 4.1.2) have been simulated, and the results are highlighted in blue in Table **5**.

Table 5. Voc, Jsc, FF, Pm, and η of CIGS Solar Cell

Dc of P-type CdTe (cm⁻³)	Dc of N-type (cm⁻³)	Jsc (mA/cm²)	Voc (V)	Pm (mW/cm²)	FF (%)	η (%)
AZO/CdS/CIGS/ZnTe						
2×10^{16}	1×10^{17}	39.07	0.66	7.63	29.39	7.63
2×10^{12}	1×10^{19}	42.05	0.70	20.92	71.19	20.9
AZO/ZnS/CIGS/ZnTe						
2×10^{16}	5×10^{15}	28.39	0.63	14.48	81.45	14.48
2×10^{19}	5×10^{14}	25.77	0.81		85.75	17.95
ITO/CdS/CIGS/ZnTe						
2×10^{16}	1×10^{17}	24.06	0.63	11.49	76.20	11.49
2×10^{16}	1×10^{20}	23.40		11.8	.45	11.8
ITO/ZnS/CIGS/ZnTe						
2×10^{16}	5×10^{15}	25.18	0.62	12.75	81.37	12.75
2×10^{19}	5×10^{15}	22.	0.81	15.77	8.4	15.77

Footnote: Dc is donor concentration, Jsc is short circuit current density, Voc is open circuit voltage, Pm is maximum power, FF is the fill factor, and η is efficiency.

Alteration of the P-type & N-type material's doping concentrations have been done in the same ranges as those of the CdTe solar cell, and the optimum results are highlighted in red in Table **5**.
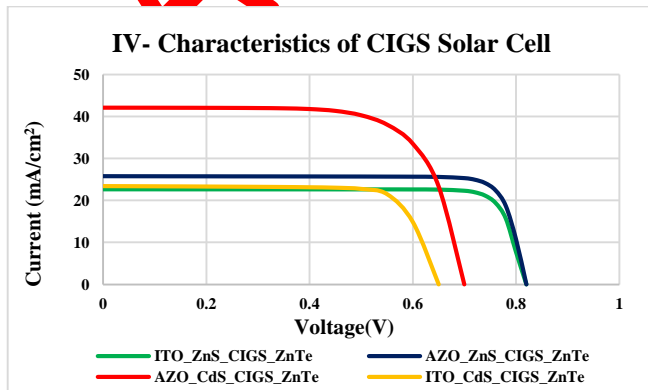

Fig.**10**. IV- Characteristics of CIGS Solar Cell

The four combinations of the CIGS solar cells' I-V curves have been drawn and shown in Fig. **10**. The AZO/CdS/CIGS/ZnTe solar cell has the best efficiency among the four combinations. The Voc, Jsc, Pm, FF, and η of the AZO/CdS/CIGS/ZnTe solar cell are 0.70 V, 42.05 mA/cm², 20.92 mW/cm², 71.19%, and 20.92% respectively. One interesting thing is, before and after optimization, the efficiency of the solar cell is 7.63% and 20.92%, respectively. Therefore, it is observed that there has been a dramatic increase in the efficiency of AZO/CdS/CIGS/ZnTe solar cells after the optimization of doping concentration. Thus, it can be said that the optimum doping concentration is one of the key factors in the design and development of a solar cell. Similar to a CdTe solar cell, a CIGS solar cell's AZO layer performs better than the ITO layer, as seen in Table **5** and Fig. **10**.

4.2.3 CZTS Solar Cell

Once again, keeping thicknesses of the TCO, buffer layer, absorber layer, and BSR layer fixed at 0.1 μm, 0.02 μm, and 2 μm respectively, this time, simulation of four combinations of CZTS solar cells was carried out first.

Table 6. Voc, Jsc, FF, Pm, and η of CZTS Solar Cell

Dc of P-type CdTe (cm⁻³)	Dc of N-type (cm⁻³)	Jsc (mA/cm²)	Voc (V)	Pm (mW/cm²)	FF (%)	η (%)
AZO/CdS/CZTS						
2×10^{14}	1×10^{17}	27.48	0.89	13.93	56.92	13.93
2×10	1×10^{18}	27.32	0.95	22.11	85.37	22.11
AZO/ZnS/CZTS						
2×10^{14}	5×10^{15}	27.97	0.88	21.15	85.90	21.15
2×10^{15}	5×10^{17}	27.89	0.95	22.85	86.44	22.85
ITO/CdS/CZTS						
2×10^{14}	1×10^{17}	24.52	0.88	18.04	83.97	18.04
2×10^{15}	1×10^{18}	24.16	0.94	19.62	85.98	19.62
ITO/ZnS/CZTS						
2×10^{14}	5×10^{15}	25.03	0.88	18.86	85.98	18.86
2×10^{15}	5×10^{15}	24.97	0.94	20.35	86.32	20.35

Footnote: Dc is donor concentration, Jsc is short circuit current density, Voc is open circuit voltage, Pm is maximum power, FF is the fill factor, and η is efficiency.

The outcomes of these four combinations have been highlighted in blue in Table **6**. Next, changes in doping concentrations of P-type & N-type layers have been made in the same ranges as those of the CdTe and CIGS solar cells, and the optimum results are highlighted in red in Table **6**.

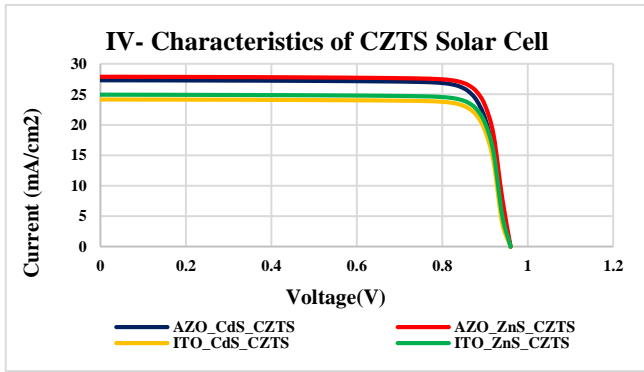Fig. **11** shows the four different I-V curve configurations for CZTS solar cells.

Fig.**11**. IV- Characteristics of CZTS Solar Cell

The solar cell made of AZO/ZnS/CZTS has the highest efficiency out of the four combinations. AZO/CdS/CZTS solar cell closely comes second in efficiency. The efficiency of these two solar cells is 22.85% and 22.11%, respectively. Because the efficiency of the AZO/CdS/CZTS solar cell is so close to that of the AZO/ZnS/CZTS solar cell, there is a probability that it will overtake the AZO/ZnS/CZTS efficiency. Nevertheless, AZO/ZnS/CZTS has the best result with Voc, Jsc, Pm, FF, and η of the solar cell are 0.95 V, 27.89 mA/cm^2, 22.85 mW/cm^2, 86.44%, and 22.85 % respectively. It is clear from Fig. **11** and Table **6** that the AZO layer performs better than the ITO layer in the CZTS solar cell.

4.3 I-V curves, Energy-Band Diagram

The best CdTe, CIGS, and CZTS models, according to sections 4.2.1, 4.2.2, and 4.2.3, are AZO/CdS/CdTe/ZnTe, AZO/CdS/CIGS/ZnTe, and AZO/ZnS/CZTS, respectively. For these three structures, I-V curves have been drawn and depicted in Fig. **12**.
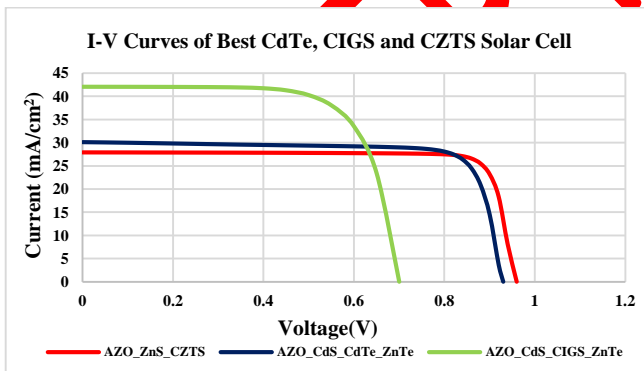

Fig. **12**. I-V Curves of Best CdTe, CIGS, and CZTS Solar Cell

Among these three structures, CZTS solar cell has the best efficiency of 22.85 %. Followed by CdTe and CIGS solar cells with 22.51% and 20.92%, respectively.

The energy-band diagram of AZO/CdS/CdTe/ZnTe, AZO/CdS/CIGS/ZnTe, and AZO/ZnS/CZTS, solar cells are sown in Fig. **13**, Fig. **14,** and Fig. **15** respectively.
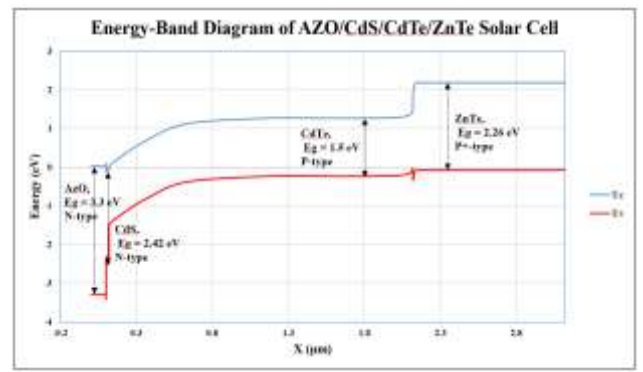

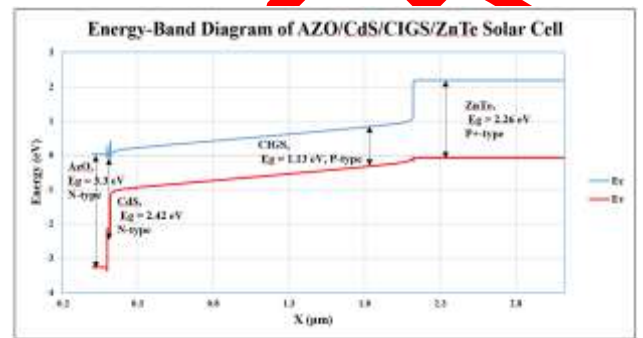Fig. **13**. Energy-Band Diagram of AZO/CdS/CdTe/ZnTe Solar Cell

Fig. **14**. Energy-Band Diagram of AZO/CdS/CIGS/ZnTe Solar Cell

The x-axis on all three energy-band diagrams indicates the thickness of each layer, and energy is shown on the y-axis in eV. The TCO and buffer layers are the first and second layers. AZO and CdS serve as the TCO and buffer layers in all three solar cells as shown in Fig. **13**, Fig. **14,** and Fig. **15**. Because the thickness of CdS is 0.02 μm, (whereas the thickness of AZO is 0.1 μm) the length of CdS appears small in the energy -band diagrams. The length of the absorbers layers (CdTe, CIGS, and CZTS) in the energy-band diagram are quite big, as all are 2 μm in length. Lastly, the ZnTe BSR layer, which has a length of 1 μm is shown in Fig. **13** and Fig. **14**. No BSR layer has been seen in Fig. **15** because CZTS lacks a ZnTe BSR layer.
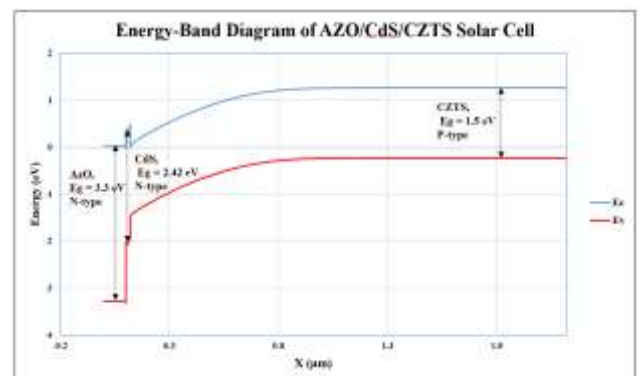

Fig. **15**. Energy-Band Diagram of AZO/CdS/CZTS Solar Cell

The energy-band diagram schematic demonstrates that there are three types of heterojunctions in Fig. **13** and Fig.

9

14 and two heterojunctions in Fig. **15**. The first two heterojunctions are formed between TCO:buffer layer and buffer layer:absorber layer. The third heterojunction is formed between the absorber layer:BSR layer and is depicted in Fig. **13** and Fig. **14**. Differences in band gaps of two different semiconductors in contact result in band edge discontinuities (band offsets) at the interface. At the heterojunction interface, there appears a discontinuity of the conduction bands ΔE_c and the valence bands ΔE_v. The ΔE_c and ΔE_v values are calculated from the energy-band diagram and are given in Table **7**.

Table 7. ΔE_c and ΔE_v values of CdTe, CIGS, and CZTS Solar Cell

Solar Cell	1st Heterojunction	2nd Heterojunction	3rd Heterojunction
CdTe	$\Delta E_c = 0.05$ $\Delta E_v = -0.93$	$\Delta E_c = -0.3$ $\Delta E_v = -0.62$	$\Delta E_c = 1.1$ $\Delta E_v = -0.34$
CIGS	$\Delta E_c = 0.05$ $\Delta E_v = -0.93$	$\Delta E_c = -0.11$ $\Delta E_v = -1.18$	$\Delta E_c = 0.91$ $\Delta E_v = 0.22$
CZTS	$\Delta E_c = 0.05$ $\Delta E_v = -0.93$	$\Delta E_c = -0.2$ $\Delta E_v = -0.72$	-

5. Discussion

In this work, initial simulations have been conducted using the reference values taken from the literature. The optimization of solar cells has been accomplished by varying the doping concentration (buffer layer and absorber layer) and TCO thickness. Significant increases in efficiency have been found after optimization (shown in Table **8**).

Table 8. Increase in efficiency after optimization

Solar Cell	Efficiency, η (%) Using reference data from the literature	Efficiency, η (%) After optimization	Increase in efficiency (%)
AZO/CdS/CdTe/ZnTe	20.18	22.51	11.55
AZO/ZnS/CdTe/ZnTe	17.88	20.19	12.92
ITO/CdS/CdTe/ZnTe	18.32	19.92	8.73
ITO/ZnS/CdTe/ZnTe	15.72	16.75	6.55
AZO/CdS/CIGS/ZnTe	7.63	20.92	174.18
AZO/ZnS/CIGS/ZnTe	14.48	17.95	23.96
ITO/CdS/CIGS/ZnTe	11.49	11.82	2.872
ITO/ZnS/CIGS/ZnTe	12.75	15.77	23.69
AZO/CdS/CZTS	13.93	22.11	58.72
AZO/ZnS/CZTS	21.15	22.85	8.038
ITO/CdS/CZTS	18.04	19.62	8.76
ITO/ZnS/CZTS	18.86	20.35	7.90

The numerical simulation demonstrates that the optimum TCO thickness is 0.1 μm. The efficiency of solar cells with AZO layers is consistently better than those with ITO layers. It may be because the AZO layer has better optical transparency and thermal stability [48]. Simulation results also show that the ITO layer overall works well with CZTS solar cells, specifically with ITO/CdS/CZTS solar cells. It is anticipated that ITO will surpass AZO's performance if suitable material, thickness, and doping concentrations are chosen. Nevertheless, the debate about the values of AZO vs. ITO for thin film solar cells is still ongoing [49]. Currently, both TCO materials are used by the manufacturers.

It has been observed from the solar cell simulations that, for most of the cases CdS buffer layer has better efficiency than its counterpart ZnS buffer layer. Although, the best efficiency has been obtained with CZTS solar cells having ZnS as the buffer layer. No clear winner can be determined in terms of the CdS or ZnS buffer layer.

According to Fig. **12**, CIGS solar cells don't perform as well as CdTe or CZTS solar cells. It may be because band gap tuning of the CIGS absorber layer has not been done here. As stated earlier, the bandgap of the CIGS layer varies from 1.1 to 1.7 eV. Here, the bandgap has been kept fixed at 1.13 eV. The efficiency of CIGS solar cells may be higher than that of CdTe or CZTS solar cells if the bandgap of the CIGS absorber layer is appropriately calibrated.

For all CdTe and CIGS solar cell combinations, it has been observed that applying the ZnTe BSR layer causes minor improvement than without the ZnTe BSR layer. However, correct thickness adjustment of ZnTe BSR is projected to provide more efficiency than without any ZnTe BSR. It should be noted that during the simulation of ZnTe as the BSR layer for CZTS solar cells unexpected error occurred; hence it has been omitted from this study. In this work, the effects of using a back-surface reflector (BSR) layer made of zinc telluride (ZnTe) have been done for CdTe and CIGS solar cells.
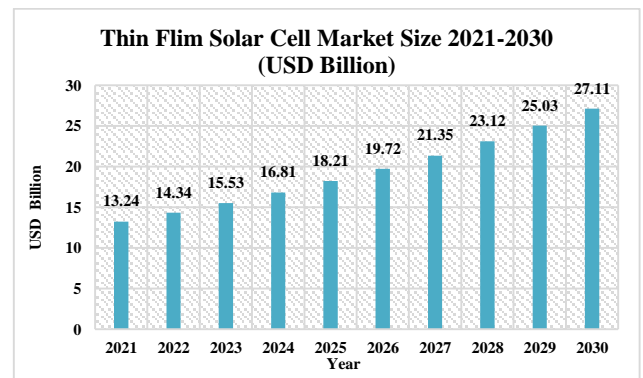

Fig. **15**. Thin Flim Solar Cell Market Size 2021-2030

The market for thin film solar cells was estimated to be worth USD 13.24 billion in 2021 and is anticipated to grow to USD 27.11 billion by 2030, as shown in Fig. **15** [50]. The vast majority of commercial thin-film modules produced worldwide are CdTe-based PV modules [51]. In

contrast, CIGS holds the second-largest market share among thin film technologies [52]. However, the efficiency of CZTS solar cells is still much lower than CdTe and CIGS PV devices. Therefore, the CZTS PV module is not available in today's market. Experimental research on CZTS solar cells is still ongoing. Currently, researchers from South Korea's Daegu Gyeongbuk Institute of Science and Technology have achieved a new efficiency record of 11.4% for a cell based on a copper zinc tin sulfide thin film applied to a flexible substrate [53]. According to Solar cell efficiency tables (Version 61), the efficiency of CdTe, CIGS, and CZTS solar cells is 22.1%, 23.35%, and 11% respectively [54]. Furthermore, the efficiency of CdTe and CIGS PV modules are 19.5% and 19.2% respectively. In this work, the best efficiency of CdTe, CIGS, and CZTS solar cells found in the simulations is 22.51%, 20.92%, and 22.85 % respectively. The efficiency of CdTe and CIGS observed in the simulation is comparable to that of CdTe and CIGS solar cells currently available. However, the efficiency of the CZTS solar cell is found higher in simulation. If the CZTS solar cell is fabricated using the simulated parameters, it is anticipated that some enhancements may be possible.

In light of the above discussion, it is experimentally feasible (or will be possible) to integrate CdTe, CIGS, and CZTS-based solar systems for use in real applications.

Crystalsol, an Austrian producer of CZTS solar cells, reported that the cost per watt for a CZTS product on a plastic substrate is $0.49 [55]. Similarly, the CIGS module manufacturing costs are presently about $0.49 per watt in the US [56]. Whereas the CdTe module production expenses in 2015 were roughly $0.46 /Watt [57] and according to NREL's forecast [58], costs will fall to $0.20 by 2025 and $0.15 by 2030. The expected reduction cost of solar cells will be due to innovations in the development and manufacturing of solar cell technology. Manufacturing solar cells at low cost and high efficiency is the main goal of photovoltaic research.

However, CdTe, CIGS, CZTS, or any other solar cell construction is intricate, and changing any of its parameters requires a lot of effort, time, and money. Furthermore, CdTe, CIGS, and CZTS solar cell fabrication processes have several steps and can be done with several equipment and techniques. All techniques have some advantages and disadvantages, as well as the equipment, may have some technological limitations. For example, the physical technique ensures a larger grain size than the chemical technique. This larger grain size affects the electrical characteristics, and in general, the larger the grain size, the more efficient the substance is. However, the physical techniques (i.e. close-spaced vapor transport (CSVT), Sputtering, etc.) are expensive and the manufacturing process is halted by the vacuum room, whereas chemical techniques (i.e. spray pyrolysis, chemical bath deposition, etc.) are less expensive but less effective. Therefore, if the technology is not mentioned, it is challenging to explain the

benefits, and drawbacks of the fabrication process. Because of this, it is essential to create an efficiency-to-cost ratio for technologies, and it needs to be high [59].

Potential future advances of thin film solar cells are quite a few. But the most prominent is semi-transparent solar cells which can be used as building windows. It is possible because very recent MIT researchers have developed a kind of ultrathin, lightweight solar cells that can be seamlessly added to any surface [60-61].

6. Conclusion

One of the main objectives of this research has been to use free software that facilitates accurate numerical simulation of CdTe, CIGS, and CZTS solar cells using the electrical and optical parameters reported in the literature. The most recent studies on simulations of CdTe, CIGS, and CZTS solar cells demonstrate efficiencies of 15%, 24.94%, and 26.53% respectively, having CdS/CdTe/Graphene (P+Type), ZnSe/CdS/CIGS/Si, and ITO/CdS/CZTS/CuS structures [62-64]. While on the contrary, in this research work, the best CdTe, CIGS, and CZTS models are for AZO/CdS/CdTe/ZnTe, AZO/CdS/CIGS/ZnTe, and AZO/ZnS/CZTS structures having efficiencies 22.51%, 20.92%, and 22.85 % respectively. The simulation results clearly show that among these three types of solar cells, the CZTS solar cell is the best. However, after optimization, all three solar cells show promising results. Thus, it is hoped that this study will help the novices, scientists, researchers, and manufacturers to understand the behavior of CdTe, CIGS, and CZTS thin-film solar cells and to fabricate high-efficiency thin-film solar cells in the near future.

Acknowledgments

References

[1] H. Heriche, Z. Rouabah, and N. Bouarissa, "New ultra-thin CIGS structure solar cells using SCAPS simulation program", *International Journal of Hydrogen Energy*, vol. 42, no. 15, pp. 9524-9532, 2017.

[2] M. Elbar and S. Tobbeche, "Numerical Simulation of CGS/CIGS Single and Tandem Thin-film Solar Cells using the Silvaco-Atlas Software", *Energy Procedia*, vol. 74, pp. 1220-1227, 2015.

[3] B. Farhadi and M. Naseri, "Structural and physical characteristics optimization of a dual junction CGS/CIGS solar cell: A numerical simulation", *Optik*, vol. 127, no. 21, pp. 10232-10237, 2016.

[4] A. Benmir and M. Aida, "Analytical modeling and simulation of cigs solar cells", *Energy Procedia*, vol. 36, pp. 618-627, 2013.

[5] R. Mohottige and S. Kalawila Vithanage, "Numerical simulation of a new device architecture for CIGS-based thin-film solar cells using 1D-SCAPS simulator", *Journal of Photochemistry and Photobiology A: Chemistry*, vol. 407, p. 113079, 2021.

[6] B. Barman and P. Kalita, "Influence of back surface field layer on enhancing the efficiency of CIGS solar cell", *Solar Energy*, vol. 216, pp. 329-337, 2021.

[7] F. Jhuma, M. Shaily, and M. Rashid, "Towards high-efficiency CZTS solar cell through buffer layer optimization", *Materials for Renewable and Sustainable Energy*, vol. 8, no. 1, 2019.

[8] F. Belarbi, W. Rahal, D. Rached, S. Benghabrit, and M. Adnane, "A comparative study of different buffer layers for CZTS solar cell using Scaps-1D simulation program", *Optik*, vol. 216, p. 164743, 2020

[9] A. Cherouana and R. Labbani, "Numerical simulation of CZTS solar cell with silicon back surface field", *Materials Today: Proceedings*, vol. 5, no. 5, pp. 13795-13799, 2018.

[10] A. Haddout, A. Raidou, and M. Fahoume, "A review on the numerical modeling of CdS/CZTS-based solar cells", *Applied Physics A*, vol. 125, no. 2, 2019.

[11] A. Bouarissa, A. Gueddim, N. Bouarissa, and H. Maghraoui-Meherezi, "Modeling of ZnO/MoS2/CZTS photovoltaic solar cell through window, buffer and absorber layers optimization", *Materials Science and Engineering: B*, vol. 263, p. 114816, 2021.

[12] K. Sreevidya, N. Abraham and C. Sajeev, "Simulation studies of CZTS thin film solar cell using different buffer layers", *Materials Today: Proceedings*, vol. 43, pp. 3684-3691, 2021.

[13] J. Duenow and W. Metzger, "Back-surface recombination, electron reflectors, and paths to 28% efficiency for thin-film photovoltaics: A CdTe case study", *Journal of Applied Physics*, vol. 125, no. 5, p. 053101, 2019.

[14] G. Hashmi, M. Imtiaz, and S. Rafique, "Towards high efficiency solar cells: composite metamaterials", *Global Journal of Researches in Engineering: Electrical and Electronics Engineering*, vol. 13, no. 10, pp. 11-16, 2013.

[15] "Photovoltaic effect | physics", Encyclopedia Britannica. https://www.britannica.com/science/photovoltaic-effect.

[16] "Absorber layer as P-type semiconductor material", ResearchGate. https://www.researchgate.net/post/In_thin_film_solar_cells_all_absorber_layers_are_p-type_what_is_the_reason.

[17] A. Teyou Ngoupo, S. Ouédraogo, F. Zougmoré, and J. Ndjaka, "New architecture towards ultrathin CdTe solar cells for high conversion efficiency", *International Journal of Photoenergy*, vol. 2015, pp. 1-9, 2015.

[18] "Cadmium Telluride Solar Cells ", Energy.gov. https://www.energy.gov/eere/solar/cadmium-telluride.

[19] M. Green, E. Dunlop, J. Hohl-Ebinger, M. Yoshita, N. Kopidakis, and X. Hao, "Solar cell efficiency tables (version 57)", *Progress in Photovoltaics: Research and Applications*, vol. 29, no. 1, pp. 3-15, 2020.

[20] I. Tinedert, F. Pezziment, M. Megherbi and A. Saadoune, "Design and simulation of a high efficiency CdS/CdTe solar cell", *Optik*, vol. 208, p. 164112, 2020.

[21] L. Nykyruy, R. Yavorskyi, Z. Zapukhlyak, G. Wisz and P. Potera, "Evaluation of CdS/CdTe thin film solar cells: SCAPS thickness simulation and analysis of optical properties", *Optical Materials*, vol. 92, pp. 319-329, 2019.

[22] D. Parashar, V. Krishna, S. Moger, R. Keshav, and M. Mahesha, "Thickness optimization of ZnO/CdS/CdTe solar cell by numerical simulation", *Transactions on Electrical and Electronic Materials*, vol. 21, no. 6, pp. 587-593, 2020.

[23] O. Shoewu, G. Anuforonini, and O. Duduyemi, "Simulation of the performance of CdTe/CdS/ZnO multi-junction thin film solar cell", *Review of Information Engineering and Applications*, vol. 3, no. 1, pp. 1-10, 2016.

[24] H. Fardi and F. Buny, "Characterization and modeling of CdS/CdTe heterojunction thin-film solar cell for high efficiency performance", *International Journal of Photoenergy*, vol. 2013, pp. 1-6, 2013.

[25] Rihana, S. Ahmed and M. Khalid, "Simulation of CIGS based solar cells with SnO_2 window layer using SCAPS-1D", *2019 International Conference on Power Electronics, Control and Automation (ICPECA)*, 2019.

[26] L. Isac, C. Cazan, A. Enesca, and L. Andronic, "Copper sulfide based heterojunctions as photocatalysts for dyes photodegradation," *Frontiers in Chemistry*, vol. 7, 2019.

[27] "Types of recombination," *PVEducation*. https://www.pveducation.org/pvcdrom/pn-junctions/types-of-recombination#:~:text=There%20are%20three%20types%20of,in%20silicon%2Dbased%20solar%20cells.

[28] "The types of recombination in semiconductors," *The Types of Recombination in Semiconductors*, 13-Oct-2022. https://resources.system-analysis.cadence.com/blog/msa2022-the-types-of-recombination-in-semiconductors.

[29] "CdTe PV modules and health risk," *HiSoUR*. https://www.hisour.com/cadmium-telluride-39637/.

[30] R. Sultana, A. Bahar, M. Asaduzzaman, M. Bhuiyan, and K. Ahmed, "Numerical dataset for analyzing the performance of a highly efficient ultrathin film CdTe solar cell", *Data in Brief*, vol. 12, pp. 336-340, 2017.

[31] S. Sundaram, K. Shanks, and H. Upadhyaya, "Thin film photovoltaics", *A Comprehensive Guide to Solar Energy Systems*, pp. 361-370, 2018.

[32] M. Asaduzzaman, M. Hasan and A. Bahar, "An investigation into the effects of band gap and doping concentration on Cu(In,Ga)Se$_2$ solar cell efficiency", *Springer Plus*, vol. 5, no. 1, 2016.

[33] M. Asaduzzaman, M. Hosen, M. Ali and A. Bahar, "Non-Toxic buffer layers in flexible Cu(In,Ga)Se$_2$ photovoltaic cell applications with optimized absorber thickness", *International Journal of Photoenergy*, vol. 2017, pp. 1-8, 2017.

[34] A. Acevedo-Luna, R. Bernal-Correa, J. Montes-Monsalve, and A. Morales-Acevedo, "Design of thin film solar cells based on a unified simple analytical model", *Journal of Applied Research and Technology*, vol. 15, no. 6, pp. 599-608, 2017.

[35] S. Fatemi Shariat Panahi, A. Abbasi, V. Ghods and M. Amirahmadi, "Analysis and improvement of CIGS solar cell efficiency using multiple absorber substances simultaneously", *Journal of Materials Science: Materials in Electronics*, vol. 31, no. 14, pp. 11527-11537, 2020.

[36] H. Heriche, Z. Rouabah and L. Selmani, "Thickness optimization of various layers of CZTS Solar Cell", *Journal of New Technology and Materials*, vol. 4, no. 1, pp. 27-30, 2014.

[37] S. Oyedele and B. Aka, "Numerical simulation of varied buffer layer of solar cells based on CIGS", *Modeling and Numerical Simulation of Material Science*, vol. 07, no. 03, pp. 33-45, 2017.

[38] R. Treharne, A. Seymour-Pierce, K. Durose, K. Hutchings, S. Roncallo and D. Lane, "Optical design and fabrication of fully sputtered CdTe/CdS solar cells", *Journal of Physics: Conference Series*, vol. 286, p. 012038, 2011.

[39] K. Sato and S. Adachi, "Optical properties of ZnTe", *Journal of Applied Physics*, vol. 73, no. 2, pp. 926-931, 1993.

[40] H. ElAnzeery et al., "Refractive index extraction and thickness optimization of Cu$_2$ZnSnSe$_4$ thin film solar cells", *Physica Status Solidi (a)*, vol. 212, no. 9, pp. 1984-1990, 2015.

[41] M. Querry, "Optical constants of minerals and other materials from the millimeter to the ultraviolet, Contractor Report CRDEC-CR-88009", *Apps.dtic.mil*, 1987.

[42] S. Sharbati, I. Gharibshahian, and A. Orouji, "Designing of AlxGa1-xAs/CIGS tandem solar cell by analytical model", *Solar Energy*, vol. 188, pp. 1-9, 2019.

[43] S. Collin et al., "Optical characterizations and modeling of semitransparent perovskite solar cells for tandem applications", *Eupvsec-proceedings.com*, 2019.

[44] Z. Holman et al., "Infrared light management in high-efficiency silicon heterojunction and rear-passivated solar cells", *Journal of Applied Physics*, vol. 113, no. 1, p. 013107, 2013.

[45] T. König et al., "Electrically tunable plasmonic behavior of nanocube–polymer nanomaterials induced by a redox-active electrochromic polymer", *ACS Nano*, vol. 8, no. 6, pp. 6182-6192, 2014.

[46] K. Shin, E. Jang, J. Cho, J. Yoo, J. Park and O. Byungsung, "Study on the fabrication of back surface reflectors in nano-crystalline silicon thin-film solar cells by using random texturing aluminum anodization", *Journal of the Korean Physical Society*, vol. 67, no. 6, pp. 1033-1039, 2015.

[47] F. Abrinaei, M. Shirazi and M. Hosseinnejad, "Investigation of growth dynamics of nanostructured aluminum doped zinc oxide thin films deposited for the solar cell applications", *Journal of Inorganic and Organometallic Polymers and Materials*, vol. 26, no. 1, pp. 233-241, 2015.

[48] G. Lee, P. M., W. Park and J. Kim, "Enhanced optical and electrical properties of ITO/Ag/AZO transparent conductors for photoelectric applications", *International Journal of Photoenergy*, vol. 2017, pp. 1-9, 2017.

[49] " Front Contact - Mustang Vac", Mustangvac.com. https://www.mustangvac.com/Front-Contact.

[50] "Thin Film Solar Cell Market," *Precedence Research*. https://www.precedenceresearch.com/thin-film-solar-cell-market.

[51] "Thin film solar PV market analysis - industry report - trends, Size & Share," *Mordor Intelligence*. https://www.mordorintelligence.com/industry-reports/global-thin-film-solar-collector-market-industry#:~:text=Thin%20Film%20Solar%20PV%20Market%20%2D%20Growth%2C%20Trends%2C%20COVID%2D,and%20Rest%20of%20the%20World).

[52] "Photovoltaics report - Fraunhofer Institute." https://www.ise.fraunhofer.de/content/dam/ise/de/documents/publications/studies/Photovoltaics-Report.pdf.

[53] M. Hutchins, "New efficiency record for flexible CZTS," *pv magazine International*, 23-Sep-2019. https://www.pv-magazine.com/2019/09/23/new-efficiency-world-record-for-flexible-czts/.

[54] M. A. Green, E. D. Dunlop, G. Siefer, M. Yoshita, N. Kopidakis, K. Bothe, and X. Hao, "Solar Cell Efficiency Tables (version 61)," *Progress in Photovoltaics: Research and Applications*, vol. 31, no. 1, pp. 3–16, 2022.

[55] A. Wang, N. L. Chang, K. Sun, C. Xue, R. J. Egan, J. Li, C. Yan, J. Huang, H. Rong, C. Ramsden, and X. Hao, "Analysis of manufacturing cost and market niches for Cu2ZnSnS4 (CZTS) solar cells," *Sustainable Energy & Fuels*, vol. 5, no. 4, pp. 1044–1058, 2021.

[56] K. A. W. Horowitz, R. Fu, and M. Woodhouse, "An analysis of glass–GLASS CIGS manufacturing costs," *Solar Energy Materials and Solar Cells*, vol. 154, pp. 1–10, 2016.

[57] "Sustainability report 2020 - First solar," *Stellenbosch University, Centre for Renewable and Sustainable Energy Studies*. https://www.firstsolar.com/en-Emea/-/media/First-Solar/Sustainability-Documents/FirstSolar_Sustainability-Report_2020.ashx.

[58] "Cadmium Telluride Accelerator Consortium," *NREL.gov*. https://www.nrel.gov/pv/cadmium-telluride-photovoltaics-accelerator-consortium-solicitation.html.

[59] A. Arce-Plaza, F. Sánchez-Rodriguez, M. Courel-Piedrahita, O. Vigil Galán, V. Hernandez-Calderon, S. Ramirez-Velasco, and M. Ortega López, "CdTe thin films: Deposition techniques and applications," *Coatings and Thin-Film Technologies*, 2019.

[60] Adam Zewe | MIT News Office, "Paper-thin solar cell can turn any surface into a power source," *MIT News | Massachusetts Institute of Technology*. https://news.mit.edu/2022/ultrathin-solar-cells-1209.

[61] C. S. Durganjali, S. Bethanabhotla, S. Kasina, and D. S. Radhika, "Recent developments and future advancements in solar panels technology," *Journal of Physics: Conference Series*, vol. 1495, no. 1, p. 012018, 2020.

[62] D. KC, D. K. Shah, M. S. Akhtar, M. Park, C. Y. Kim, O.-B. Yang, and B. Pant, "Numerical investigation of graphene as a back surface field layer on the performance of Cadmium Telluride Solar Cell," *Molecules*, vol. 26, no. 11, p. 3275, 2021.

[63] M. Belarbi, O. Zeggai, and S. Louhibi-Fasla, "Parameters optimization of heterojunction ZnSe/cds/CIGS/si solar cells using SCAPS-1D software," *Journal of Renewable Energies*, 2022.

[64] A. Hosen, B. Islam, H. Khatun, M. S. Islam, K. M. S. Rahmotullah, and S. R. Al Ahmed, "Device simulation of a highly efficient CZTS solar cell with CUS as hole transport layer," *2021 IEEE International Conference on Telecommunications and Photonics (ICTP)*, 2021.